Journal of Colloid and Interface Science 362 (2011) 430–438

Contents lists available at ScienceDirect

Journal of Colloid and Interface Science

www.elsevier.com/locate/jcis

Light and host–guest inclusion mediated salmon sperm DNA/surfactant interactions

Yiyang Lin [a], Yudong Zhang [a], Yan Qiao [a], Jianbin Huang [a,*], Baocai Xu [b]

[a] Beijing National Laboratory for Molecular Sciences (BNLMS), State Key Laboratory for Structural Chemistry of Unstable and Stable Species, College of Chemistry and Molecular Engineering, Peking University, Beijing 100871, China
[b] School of Chemical and Environmental Engineering, Beijing Technology & Business University, Beijing 100037, China

ARTICLE INFO

Article history:
Received 27 April 2011
Accepted 30 June 2011
Available online 13 July 2011

Keywords:
DNA complexation
Surfactant
Light
Host–guest interaction
Azobenzene

ABSTRACT

DNA/cationic surfactant interaction is relevant from the viewpoint of gene therapy, where the complexation and resulting compaction are essential to protect DNA from nuclease, and to allow entry of DNA into cells. In this work, light input and host–guest inclusion controlled DNA complexation by a novel cationic surfactant 1-[6-(4-phenylazo-phenoxy)-hexyl]-3-methylimidazolium bromide (AzoC6Mim) is reported. The surfactant is covalently attached with an azobenzene group, which undergoes reversible photoisomerizations by changing light input. Under visible light, *trans*-AzoC6Mim can bind to salmon sperm DNA through electrostatic attraction and hydrophobic interaction, resulting into DNA compaction. Under UV light, although *cis*-AzoC6Mim still binds to DNA chain, DNA/surfactant complex is decompacted owing to the decrease of surfactant hydrophobicity. On the other hand, azobenzene group can form an inclusion complex with α-CD through host–guest interaction, which removes AzoC6Mim from DNA chain and decompacts the DNA/surfactant complex.

1. Introduction

Gene therapy is demonstrated to be an effective approach to treat acquired and inherited diseases by transfection, which is based on the vectorization of genes to target cells and subsequent expression, that is, ferrying a correct copy of the defective gene into the cell [1]. Viruses are the most effective transfection agents *in vivo*, but their application is not without risk for patients [2]. On the other hand, the delivery of therapeutic nucleotides using non-viral vectors such as surfactants or lipids, polymers, dendrimers, and nanoparticles is attracting increasing attention [3–8]. In particular, synthetic cationic surfactants are also effective in transfection and are involved in current clinical trials based on gene therapy. The concept of gene transfection by cationic surfactants or surfactant aggregates is attractive owing to its advantages of nonimmunicity and the potential for transferring and expressing large pieces of DNA into cells.

Many factors are reported to affect efficient gene transfection including the type of nanoscale structure and the surface charge of DNA/surfactant complex. It is realized that strong DNA/cationic surfactant interaction can help to compact DNA, yielding complexes of small size [9–12]. The compaction of DNA into small particles can protect DNA from degradation by nucleases as well as facilitate cell uptake and gene transfection. Normally surfactant mediated DNA compaction exhibits a discrete first-order phase transition between an elongated coil state and a compacted globule state. The cooperative binding of cationic surfactants on DNA chains is primarily driven by both electrostatic attraction and hydrophobic effect. The cationic surfactant can be varied by the molecular structures including conventional single-tailed surfactants [13–22], Gemini surfactants [23–31], double-tailed surfactants [32–35], etc.

On the other hand, the decompaction and release of DNA from vectors inside the cells can recover the DNA properties so as to proceed to the following transcription. Therefore, precise control of DNA decompaction and release also bears great importance to gene expression. For example, Mel'nikova and Lindman reported pH-controlled DNA condensation by dodecyldimethylamine oxide surfactant [36]. Kostiainen and Rosilo used polylysine dendrons bearing cleavable disulfide linkers to perform binding and release of DNA [37]. Smith demonstrated that using a chemically degradable dendron framework allows multivalent binding to be switched off, with subsequent loss of affinity for DNA [38]. Lynn and Abbott reported the reversible condensation of DNA using a redox-active surfactant [39]. Compared with the other external stimuli to trigger DNA decompaction and release, light input is considered to be advantageous benefitting from its capability of remote control [40–42]. For example, Lee developed a means to control DNA compaction and gene delivery by light input in cationic or cationic-anionic surfactant system [43,44]. Andreasson and coworkers described the photo-switched DNA-binding of a spiropyran amphiphile [45].

Inspired by these considerations, we are particularly interested in the precise control of DNA/cationic surfactant interaction using

* Corresponding author. Fax: +86 10 62751708.
E-mail address: JBHuang@pku.edu.cn (J. Huang).

0021-9797/$ - see front matter © 2011 Elsevier Inc. All rights reserved.
doi:10.1016/j.jcis.2011.06.083

external stimuli. In this work, a cationic surfactant AzoC6Mim bearing azobenzene group is synthesized and the molecular interaction between salmon sperm DNA and AzoC6Mim is investigated. Light-responsive azobenzene group is modified on surfactant so that we can mediate surfactant/DNA interaction by light input. Also azobenzene group is supposed to increase the hydrophobic effect of surfactant, which may enhance the interaction between DNA and surfactant. A quaternized imidazolium group is attached to surfactant skeleton as the hydrophilic positive-charged group. Imidazole-type amphiphiles have recently attracted extensive attention because they can serve as both ionic liquids and surfactants. Meanwhile imidazole is a cationic planar group which may intercalate between two adjacent base pairs in duplex DNA. By using dynamic light scattering (DLS), UV–vis spectra, fluorescence probe technique, and confocal laser scanning microscopy (CLSM), photo-controlled DNA/surfactant complexation is investigated with the irradiation of UV or visible light. Moreover, the azobenzene group can form an inclusion complex with α-CD through host–guest interaction, which is exploited to realize the decompaction of DNA/surfactant complex. The possible scheme of light and host–guest inclusion controlled DNA/surfactant interaction is illustrated.

2. Materials and methods

2.1. Materials

Low-molecular-weight salmon sperm DNA from Fluka BioChemika Co. was used without further purification. DNA stock solution was freshly prepared by dissolving dried DNA in 10 mM Tris HCl buffer (pH 7.0). The concentration of DNA was determined by measurements of UV absorbance assuming the molar extinction coefficient ε_{260nm} = 6600 M^{-1} cm^{-1} expressed in nucleotide phosphates. All experiments were performed using Millipore Milli-Q deionized water (18.2 MΩ/cm resistivity).

2.2. Surfactant synthesis

The cationic surfactant AzoC6Mim is synthesized as following (Scheme 1):

(1) [4-(6-Bromo-hexyloxy)-phenyl]-diazene: 1,6-dibromohexane (19.5 g, 80 mmol) and sodium hydroxyl (0.4 g, 10 mM) was added into 50 mL THF in a flask. To this mixture, 4-phenylazo-phenol (1.98 g, 10 mmol) in 20 mL THF was added dropwise with magnetic stirring. The solution was refluxing for 24 h under N_2 protection. Finally the solvent was removed and the combined mixture was purified by recrystallization three times from THF/hexane.

(2) 1-[6-(4-Phenylazo-phenoxy)-hexyl]-3-methylimidazolium bromide (AzoC6Mim): Excess 1-methylimidazole and [4-(6-bromo-hexyloxy)-phenyl]-diazene was added to THF in a flask. The mixture was kept stirring for 24 h at 60 °C. After cooling to room temperature, the yellow solid was precipitated from the solution. This product was further recrystallized three times from acetone–ethanol and dried under vacuum. Elemental analysis calcd (%) for $C_{22}H_{27}BrN_4O{\cdot}H_2O$: C 57.27, H 6.34, N 12.14; found: C 57.23, H 6.34, N 12.12. ^{1}H NMR (400 MHz, D_2O): δ (ppm) 8.60 (s, 1H), 7.57 (m, 4H), 7.35 (m, 1H), 7.22 (m, 4H), 6.61 (s, 2H), 3.90 (t, 2H), 3.81 (s, 3H), 3.47 (t, 2H), 1.50 (m, 2H), 1.36 (m, 2H), 1.01 (m, 4H).

2.3. UV–vis absorbance

The turbidity of DNA/surfactant solution was obtained from UV–vis absorbance measurements, which were carried out on the spectrophotometer (Cary 1E, Varian Australia PTY Ltd.) equipped with a thermostated cell holder. The UV–vis measurements were conducted at 25 °C.

2.4. Dynamic light scattering

To prepare dust-free solutions for light scattering measurements, the solutions were filtered through a 0.45-μm membrane filter of hydrophilic PVDF into light scattering cells before the measurements. The light scattering cells had been rinsed with distilled acetone to ensure a dust-free condition before use. DLS was performed with a spectrometer (ALV-5000/E/WIN Multiple Tau Digital Correlator) and a Spectra-Physics 2017 200 mW Ar laser (514.5 nm wavelength). The scattering angle was 90°, and the intensity autocorrelation functions were analyzed by using the methods of Contin. In our experiment, the surfactant solutions and DNA solutions were filtered individually to prepare dust-free solution, which was further mixed carefully to obtain the desired DNA/surfactant solution.

2.5. Photoisomerization experiment

For light-triggered azobenzene *trans/cis* isomerization, surfactant or DNA/surfactant solutions were irradiated with 365 nm UV light from a Spectroline FC-100F fan-cooled, long wave UV lamp. The power of the mercury arc lamp was 100 W. The samples were

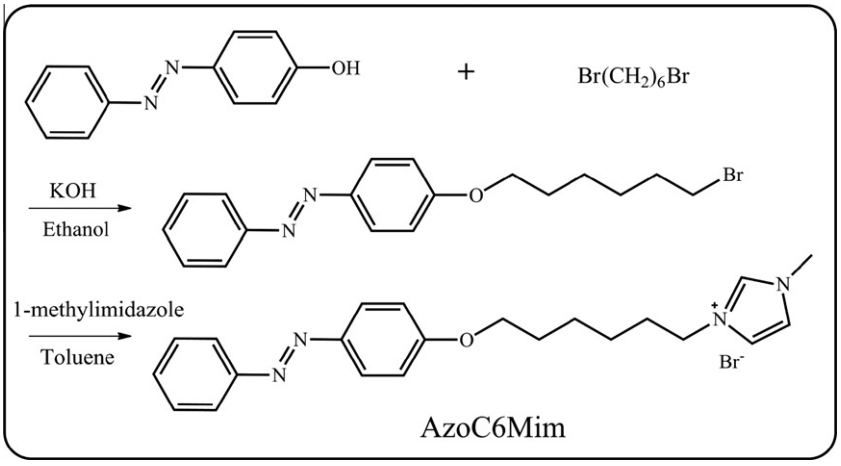

Scheme 1. Organic synthesis of cationic surfactant AzoC6Mim.

placed in a quartz tube, and the distance between the sample and light source was fixed at 15 cm. The photoisomerization could be finished within 30 min. For *cis*/*trans* transition, irradiation by visible light was performed using a 200-W incandescent light bulb (>440 nm).

2.6. Fluorescence measurement

Steady-state fluorescence spectrum was obtained with an Edinburgh FLS920 fluorescence spectrophotometer. Fluorescent probe, Nile Red (NR) or Ethidium Bromide (EB), was added into surfactant solution with the concentration of 5.0 μM (Scheme 2). The excitation wavelength of Nile Red and Ethidium Bromide was 575 nm and 546 nm respectively. Nile Red and Ethidium Bromide was chosen as the probe because its excitation peak occurs at a long wavelength where the absorption by the azobenzene group is minimal and also because its emission is very environment-sensitive. Nile Red is highly hydrophobic and poorly soluble in water. The fluorescence emission of Nile Red is strongly quenched and red-shifted in aqueous solution. However, in hydrophobic environments, Nile Red fluorescence intensity is greatly enhanced, and its emission peak shifts to a shorter wavelength [46–48].

2.7. Confocal laser scanning microscopy (CLSM)

The CLSM observation of DNA/surfactant complex was carried out in the presence of hydrophobic dye of Nile Red, which was prepared through the following process: 10 μL stock solution of Nile Red in ethanol (2.5 mM) was added to a test tube, followed by volatilization of the ethanol. Then a desired amount of surfactant solution (1 mL) was fed into the test tube with magnetic stirring. All the samples were allowed for 2 h equilibrium before CLSM observation. The solutions containing Nile Red were dropped onto a pre-cleaned glass surface, which was covered by microscope slide glass. The edge of the slide was sealed to avoid water evaporation. CLSM observation was conducted on a Leica Tcs-sp confocal laser scanning microscope.

3. Results and discussion

3.1. Photoisomerization of cationic surfactant AzoC6Mim

The azobenzene group of AzoC6Mim can realize *trans*–*cis* conformational change [49–55], which is confirmed by UV–vis spectrum (Fig. 1). Before irradiation, the spectrum is dominated by the 344 nm absorption which is ascribed to π–π^* absorption band of *trans*-azobenzene moiety. As UV irradiation proceeds, the 344 nm absorption band decreases with concomitant increase of the π–π^* and n–π^* bands of the *cis* isomer at around 316 nm and 434 nm, respectively. Moreover, the *trans*/*cis* conformational change of azobenzene can be reversibly conducted as indicated by UV–vis absorbance (Fig. S1).

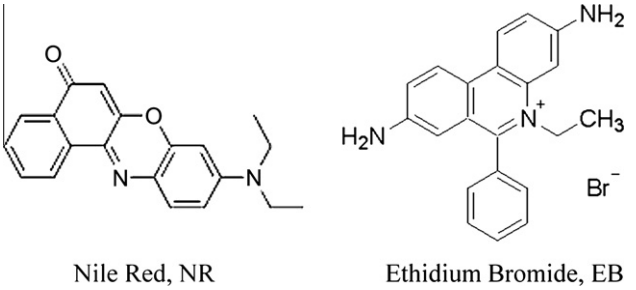

Nile Red, NR Ethidium Bromide, EB

Scheme 2. Molecular structure of Nile Red and Ethidium Bromide.

The critical micellar concentration (CMC) of AzoC6Mim is measured using Nile Red fluorescence [54]. Under visible light, the maximum emission wavelength undergoes a plateau at low AzoC6Mim concentration but runs downwards as the concentration increased above 2 mM (Fig. 2a). The concentration of 2 mM is therefore defined as CMC. A similar CMC value can be obtained from fluorescence intensity profile (Fig. 2b). After UV light irradiation, the CMC of *cis*-AzoC6Mim is found to be ~9 mM (Fig. 3a and b). It is concluded that *trans*-AzoC6Mim is more hydrophobic than *cis*-AzoC6Mim and efficient to aggregate in water. This is because *trans*-azobenzene has no dipole moment while the dipole moment of *cis*-azobenzene is 3.0 D [56,57].

3.2. Light-mediated DNA/AzoC6Mim complexation

The cationic surfactant AzoC6Mim is further used to compact salmon sperm DNA. Dynamic light scattering is employed to investigate the complexation process in DNA/AzoC6Mim solution. As shown in Fig. 4a, the apparent hydrodynamic radius distribution of DNA solution gives two separated decay modes: a slow mode and a fast mode. The fast mode with the apparent radius of 4 nm is corresponding to the rotational diffusion mode and other intermolecular diffusion mode of DNA chain, which may originate from the DNA flexibility and other intramolecular interference effect [58]. The slow mode at 155 nm can be ascribed to the translational diffusion mode of DNA chains. With the addition of 0.3 mM AzoC6Mim, the slow mode of 155 nm decreases to 132 nm, which is indicative of DNA compaction [21,59]. Meanwhile the fast mode at 4 nm disappears resulting from the compaction of DNA chains and the lack of DNA flexibility. When AzoC6Mim concentration increases to 0.5 mM, the slow mode decreases to 96 nm. When AzoC6Mim concentration reaches 0.7 mM, the DNA chains are further compacted with apparent hydrodynamic radius decreases to 67 nm. Meanwhile, an additional diffusion mode at 233 nm is observed, which may be owing to the aggregation of DNA/surfactant complexes. When surfactant concentration exceeds 0.7 mM, the solution is turbid and DLS is not applicable. The DNA/AzoC6Mim complexation can be also reflected from solution turbidity change (Fig. 4b). The turbidity of DNA solution is relatively low when surfactant concentration is below 0.7 mM; however, the solution turbidity begins to increase abruptly when AzoC6Mim concentration is above 0.7 mM. The rapid increase of solution turbidity is ascribed to the aggregation of compacted DNA/surfactant complexes. This is in agreement with DLS result. Confocal laser scanning microscopy (CLSM) image also confirms the existence of large particles resulting from aggregation of DNA/AzoC6Mim complex (1 mM/0.7 mM) (Fig. S2).

The DNA/AzoC6Mim complexation can be mediated by light irradiation benefitting from azobenzene photoisomerization. Under visible light, the addition of *trans*-AzoC6Mim to DNA solution causes solution turbidity to rise owing to DNA compaction and aggregation (Fig. 5a). After UV light irradiation, however, the DNA/AzoC6Mim solution is clear and the solution turbidity maintains unchanged. It is therefore suggested that DNA/*cis*-AzoC6Mim complexation is weak. If visible light is further applied, *cis*-AzoC6Mim transforms into *trans*-AzoC6Mim and solution turbidity increases again. The light-mediated DNA/surfactant complexation can be repeatedly switched as indicated from Fig. 5b.

To understand DNA/AzoC6Mim interaction, fluorescence technique with hydrophobic Nile Red as a probe is employed. As mentioned above, the fluorescence emission of Nile Red probe is sensitive to environmental polarity. Under visible light, the addition of 0.2 mM *trans*-AzoC6Mim into 1.0 mM DNA solution can result into the decrease of maximum emission wavelength from 652 nm to 641 nm (Fig. 6a). Because the CMC of *trans*-AzoC6Mim is about 2 mM, the remarkable blue shift of Nile Red maximum

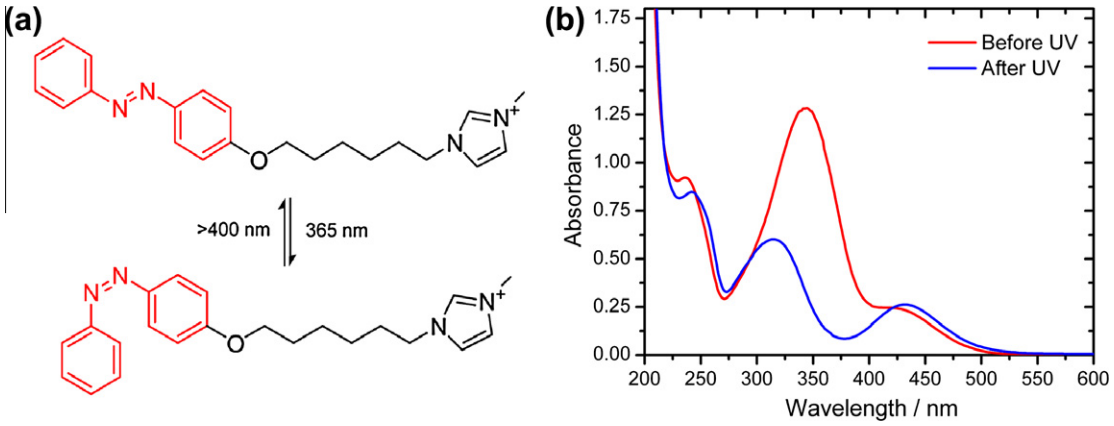

Fig. 1. (a) Molecular structure of AzoC6Mim undergoing *trans–cis* conformational transition; (b) UV–vis absorbance of AzoC6Mim aqueous solution before and after UV irradiation ([AzoC6Mim] = 0.1 mM).

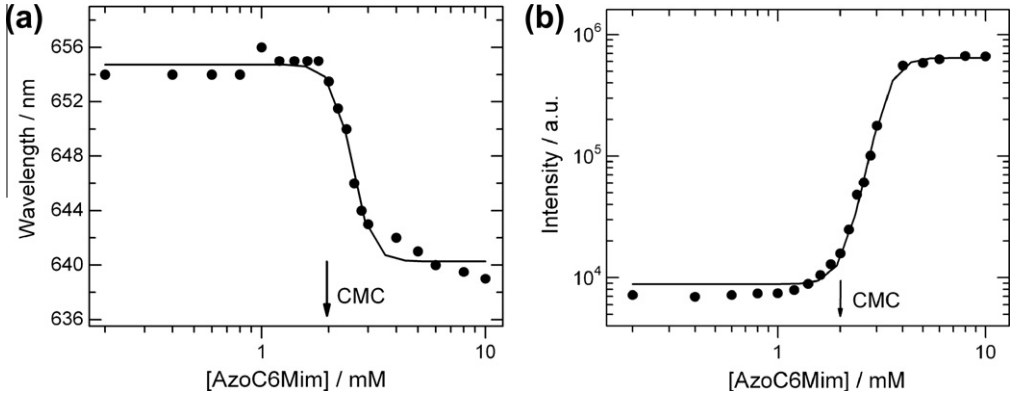

Fig. 2. (a) Maximum emission wavelength and (b) fluorescence intensity of Nile Red in AzoC6Mim solution under visible light.

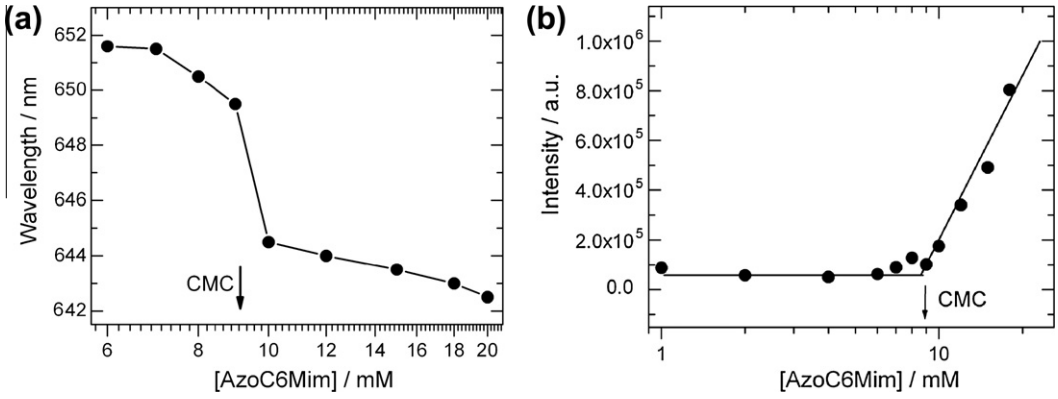

Fig. 3. (a) Maximum emission wavelength and (b) fluorescence intensity of Nile Red in AzoC6Mim solution after UV irradiation.

emission wavelength cannot be simply ascribed to the formation of *trans*-AzoC6Mim aggregates. Rather it is a consequence of hydrophobic domain formation resulting from DNA/surfactant complexation. Further addition of AzoC6Mim (>0.2 mM) does not alter the maximum emission wavelength any more, which suggests that the microenvironmental polarity of Nile Red does not significantly change. After UV light illumination, however, the maximum emission wavelength of Nile Red in DNA solution only shows slight decrease by adding *cis*-AzoC6Mim indicating the polarity of Nile Red surroundings does not markedly change. The fluorescence intensity results of Nile Red can also come to the same conclusion (Fig. 6b). Under visible light, Nile Red fluorescence in DNA solution increases by almost one order of magnitude with the addition of 0.2 mM AzoC6Mim (Fig. 6b). This implies that the microenvironment around fluorescence probe is becoming more hydrophobic owing to the formation of hydrophobic domain. When the surfactant concentration is above 0.2 mM, the fluorescence intensity profile rises relatively slowly. Under UV light, in contrast, fluorescence intensity is much lower and stays almost unchanged with the addition of AzoC6Mim. Therefore, it can be proposed that no hydrophobic domain is formed in DNA solution in the presence of *cis*-AzoC6Mim.

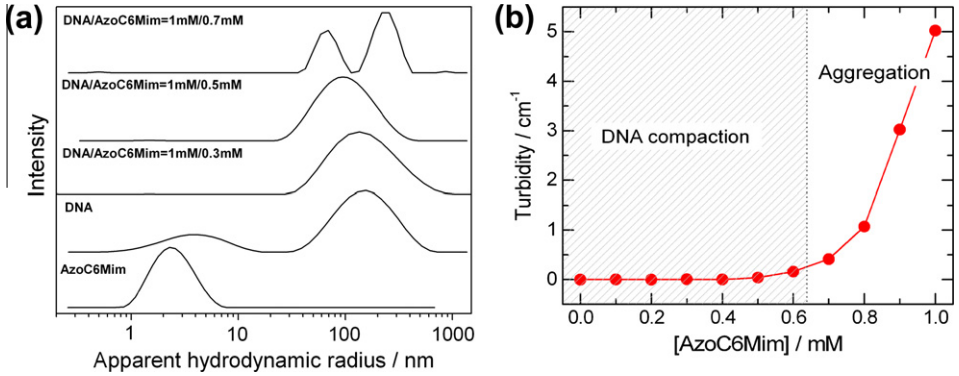

Fig. 4. (a) DLS and (b) turbidity curve of DNA/AzoC6Mim solution with the addition of AzoC6Mim under visible light ([DNA] = 1.0 mM).

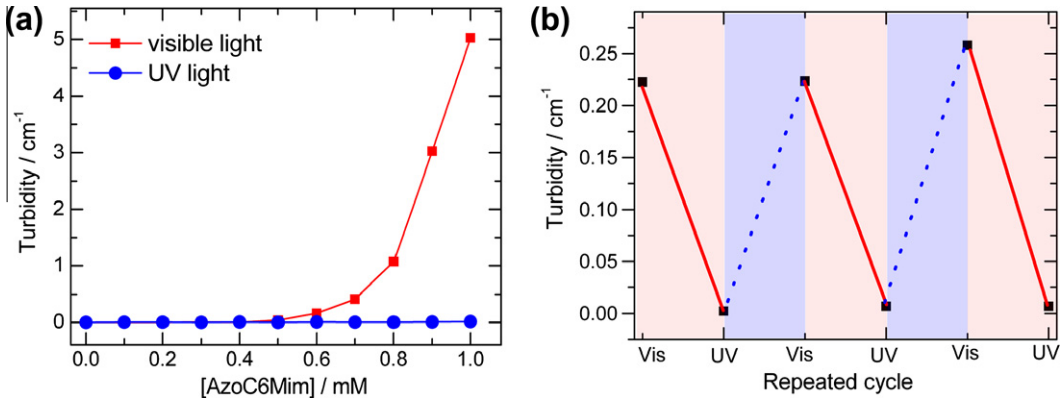

Fig. 5. (a) Turbidity of DNA/AzoC6Mim solution under visible or UV light irradiation; (b) repeated turbidity of DNA/AzoC6Mim (1.0 mM/0.5 mM) solution at 600 nm.

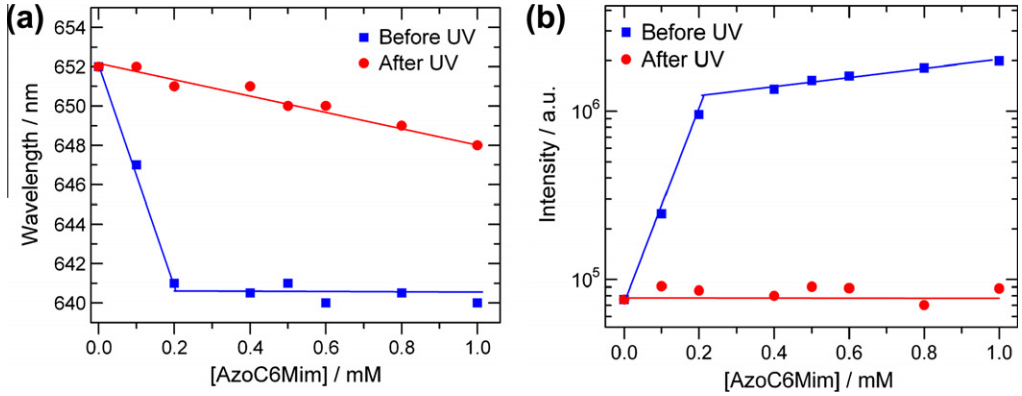

Fig. 6. (a) Maximum emission wavelength and (b) fluorescence emission intensity of Nile Red in DNA/AzoC6Mim solution under visible or UV light irradiation ([DNA] = 1.0 mM).

As proposed by the above results, cationic *trans*-AzoC6Mim will bind to DNA chain, resulting into DNA compaction under visible light. Meanwhile a hydrophobic domain will form to host hydrophobic Nile Red. As a consequence, the maximum emission wavelength runs down and the fluorescence emission intensity rises with the addition of 0.2 mM AzoC6Mim. Further addition of AzoC6Mim will reduce the surface charge density of DNA/*trans*-AzoC6Mim complex and cause the aggregation of DNA/surfactant complex, which leads to solution turbidity increase ($c > 0.7$ mM) [16,60]. Under UV light illumination, *cis*-AzoC6Mim is dominant in solution and the DNA compaction is inhibited. Yet, it remains ambiguous on the issue of DNA/AzoC6Mim interaction. In particular, it is unknown whether *cis*-AzoC6Mim binds to DNA chain under UV light irradiation.

Herein fluorescence emission of ethidium bromide is studied to give additional information of DNA/surfactant interaction under UV or visible light. Unlike Nile Red, ethidium bromide (EB) is a planar compound bearing positive charge (Scheme 2) which can intercalate between two adjacent base pairs in duplex DNA [61–66]. The fluorescence intensity of this probe increases remarkably upon the intercalation because the hydrophobic microenvironment found between base pairs protects the probe from water and molecular oxygen that may quench its fluorescence emission [67]. As shown in Fig. 7, under visible light illumination, the addition of AzoC6Mim into DNA solution cause a decrease of EB emission intensity followed by a further increase of fluorescence emission. This can be explained that the intercalation of EB into

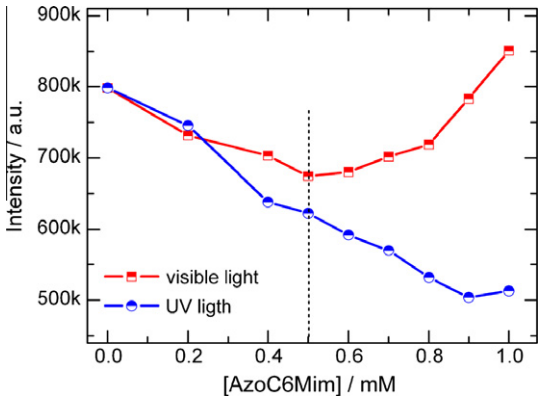

Fig. 7. Fluorescence intensity of EB in the system of DNA/AzoC6Mim solution under visible or UV light irradiation ([DNA] = 1.0 mM).

DNA double helix is excluded by *trans*-AzoC6Mim, which releases EB probe from DNA helix into bulk aqueous solution. As a result, a drop of fluorescence intensity is detected. With further addition of surfactant AzoC6Mim (>0.5 mM), EB probe penetrates into hydrophobic domain formed by DNA/*trans*-AzoC6Mim complex. Therefore, the fluorescence intensity rises gradually (Fig. 7). Under UV light illumination, the fluorescence of EB decreases continuously with the addition of *cis*-AzoC6Mim. This makes it clear that *cis*-AzoC6Mim does bind to DNA chain, which repels EB probe from DNA helix into aqueous solution. Consequently, EB fluorescence in DNA solution decreases with the addition of *cis*-AzoC6Mim. Besides, the fact that there is no turning point in fluorescence intensity profile in DNA/*cis*-AzoC6Mim solution indicates that EB does not get into a hydrophobic domain at higher AzoC6Mim concentration. This is because *cis*-AzoC6Mim cannot induce DNA compaction as well as hydrophobic domain formation.

Combined with the above results, the interaction between DNA and AzoC6Mim can be illustrated in Scheme 3. Under visible light irradiation, cationic surfactant *trans*-AzoC6Mim will bind to the DNA chain and result into DNA compaction, which benefit from hydrophobic effect and electrostatic attraction between AzoC6Mim quaternized headgroups and DNA phosphate groups. Under UV light irradiation, *trans*-AzoC6Mim transforms into *cis*-AzoC6Mim which is more hydrophilic as suggested by CMC result. Although *cis*-AzoC6Mim can bind to DNA chain, the DNA/*cis*-AzoC6Mim complex is less hydrophobic and DNA compaction is not favored.

3.3. Host–guest inclusion of AzoC6Mim with α-CD

zCyclodextrins (CDs) are known to encapsulate hydrophobic guests with suitable size and shape in the cavity. β-CD, which has an inner cavity of about 270 $Å^3$ can accommodate 8–10 CH_2 groups in a bended conformation [68,69]. α-CD, which has a larger cavity, can host *trans*-azobenzene group through host–guest interaction [70–72]. To reveal the *trans*-AzoC6Mim/α-CD association, UV–vis absorption of AzoC6Mim is measured at the same concentration by varying α-CD concentration. As shown in Fig. 8a, the UV–vis absorbance peak of *trans*-AzoC6Mim exhibits red shift with the addition of α-CD. Meanwhile the absorption at 344 nm is enhanced after association with α-CD, which is a consequence of azobenzene/α-CD inclusion. The association constant between AzoC6Mim and α-CD in aqueous solution can be determined by following the UV absorption at 344 nm. With an assumption of a 1:1 stoichiometry, the inclusion complexation of α-CD with AzoC6Mim is expressed by the following equation [70]:

$$K_a = \frac{[\text{AzoC6Mim} \cdot \text{CD}]}{[\text{AzoC6Mim}] * [\text{CD}]}$$

The double reciprocal plot is employed according to the modified Hildebrand–Benesi equation:

$$\frac{1}{\Delta A} = \frac{1}{K_a \Delta\varepsilon [\text{AzoC6Mim}][\text{CD}]_0} + \frac{1}{\Delta\varepsilon [\text{AzoC6Mim}]} = \frac{k}{[\text{CD}]_0} \frac{1}{\Delta\varepsilon [\text{AzoC6Mim}]}$$

Herein ΔA is the absorbance change before and after α-CD addition. $\Delta\varepsilon$ denotes the difference of the molar extinction coefficient between azobenzene and azobenzene/α-CD complex. The association constant K_a is calculated by the equation:

$$K_a = \frac{1}{k * \Delta\varepsilon * [\text{AzoC6Mim}]}$$

where k can be calculated from the slope value of line plot in Fig. 8b. The value of K_a is calculated to be $3.4 \times 10^4\ M^{-1}$ which is close to the value in the Ref. [70].

3.4. Host–guest interaction controlled DNA/AzoC6Mim complexation

In this work, host–guest inclusion between azobenzene and α-CD is exploited to mediate the DNA/AzoC6Mim interaction [73,74]. As shown in Fig. 9a, the DNA/AzoC6Mim solution (1 mM/1 mM) becomes transparent gradually with the addition of α-CD, which is indicative of DNA/surfactant complexes dissolution. The threshold α-CD concentration for which the solution turbidity levels off is about 1.5 mM. The fluorescence probe technique is further performed to reveal the effect of α-CD on DNA/AzoC6Mim complex. The fluorescence emission intensity of Nile Red in DNA solution lowers down (Fig. 9b) and maximum emission wavelength increases (Fig. 9c) with the addition of α-CD, suggesting Nile Red transfers to relatively hydrophilic environment. This is because: (1) in the absence of α-CD, Nile Red will locate at the hydrophobic

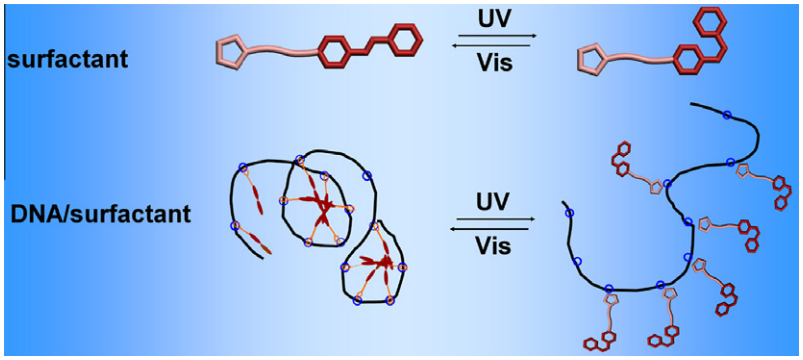

Scheme 3. Light-mediated salmon sperm DNA/AzoC6Mim interactions.

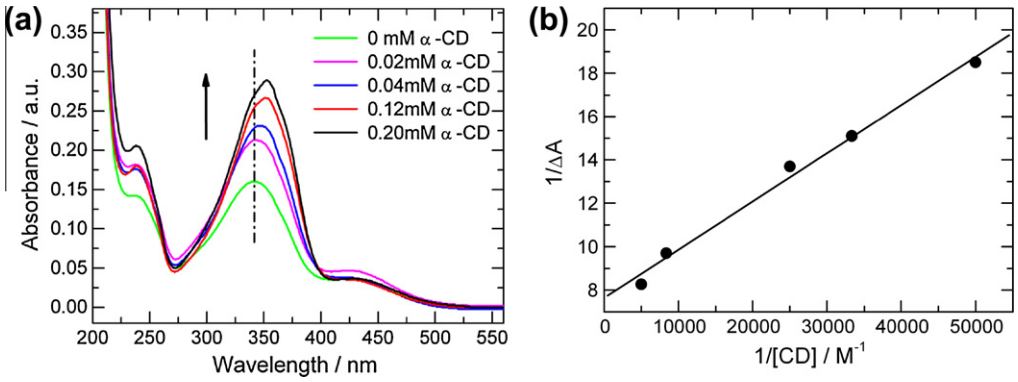

Fig. 8. (a) UV–vis spectrum of AzoC6Mim/α-CD solution. The arrow indicates the increase of α-CD concentration. (b) The profile of 1/△A versus 1/[α-CD] ([AzoC6Mim] = 0.1 mM).

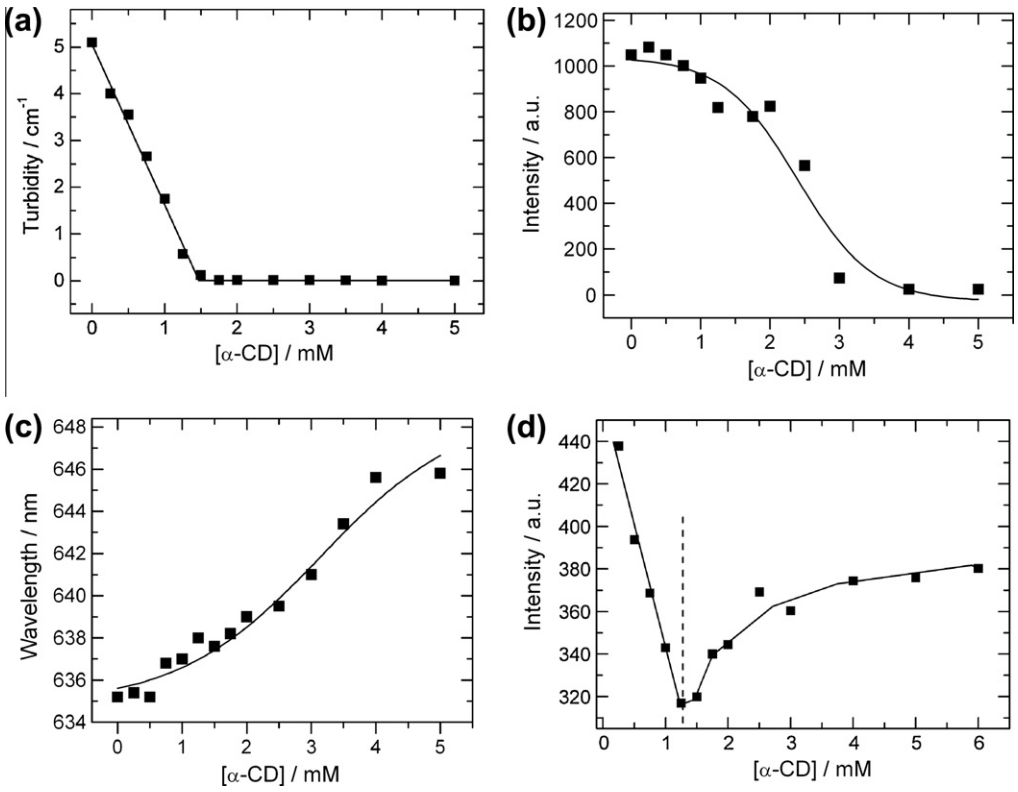

Fig. 9. Effect of α-CD on DNA/AzoC6Mim (1.0 mM/1.0 mM) solution: (a) solution turbidity; (b) fluorescence emission intensity and (c) maximum emission wavelength of Nile Red; (d) fluorescence emission intensity of EB.

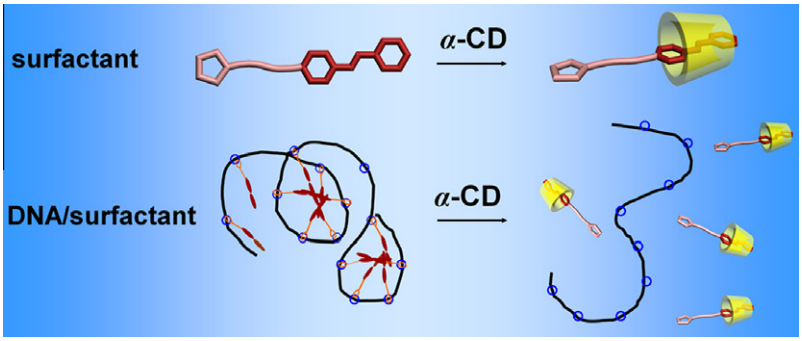

Scheme 4. Host–guest inclusion mediated DNA/surfactant interactions.

domain formed by DNA/AzoC6Mim complex; (2) in the presence of α-CD, azobenzene group will form inclusion complex with α-CD, which increases the hydrophilicity of AzoC6Mim and makes AzoC6Mim depart from the DNA. As a consequence, DNA chain is decompacted, the hydrophobic domain disappears, and Nile Red is expelled into bulk aqueous solution, resulting into the decrease of fluorescence intensity and increase of maximum emission wavelength.

On the other hand, the addition of α-CD will result into decrease of EB fluorescence in DNA/AzoC6Mim (1 mM/1 mM) solution, followed by an abrupt increase (Fig. 9d). This can be explained as following: (1) In the absence of α-CD, EB probe locates at the hydrophobic domain formed by DNA/AzoC6Mim complex. (2) With the addition of α-CD, the formation of AzoC6Mim/α-CD inclusion makes cationic surfactant more hydrophilic and cause the disappearance of hydrophobic domain. Then EB probe is expelled from DNA/AzoC6Mim hydrocarbon domain into hydrophilic aqueous environment, which quenches the EB fluorescence emission. Meanwhile, the enhancement of hydrophilicity makes AzoC6Mim leave from anionic DNA site. (3) When α-CD concentration is further increased, more AzoC6Mim will depart from DNA and the anionic residual sites on DNA chain increase. Consequently, cationic EB will intercalate into the DNA duplex resulting into fluorescence enhancement of EB (Fig. 9d). The decompaction effect of α-CD on DNA/AzoC6Mim is illustrated in Scheme 4. The decompaction of DNA/AzoC6Mim complex can be seen from DLS result, in which the particle size changes from 96 nm (without α-CD) to 145 nm (with α-CD).

4. Conclusion

In conclusion, light input and host–guest interaction controlled salmon sperm DNA/AzoC6Mim complexation is reported. Under visible light, *trans*-AzoC6Mim can interact with DNA through electrostatic attraction and hydrophobic interactions which results into the DNA compaction. Under UV light, *cis*-AzoC6Mim can still bind to DNA chain. However, DNA/*cis*-AzoC6Mim is more hydrophilic which cause the decompaction of DNA/surfactant complex. On the other hand, azobenzene group can form an inclusion complex with α-CD through host–guest interactions, which can be utilized to realize the decompaction of DNA/surfactant complex. This is because surfactant/α-CD complex is more hydrophilic and will leave the DNA chain resulting into DNA decompaction. It is hopeful that this work can give better understanding of DNA/surfactant interaction and provide an avenue toward DNA therapy using synthetic surfactant.

Acknowledgments

This work is supported by National Natural Science Foundation of China (20873001, 20633010, 50821061, 20976003 and 21073006) and National Basic Research Program of China (Grant No. 2007CB936201).

Appendix A. Supplementary material

Supplementary data associated with this article can be found, in the online version, at doi:10.1016/j.jcis.2011.06.083.

References

[1] W.F. Anderson, Science 226 (1984) 401.
[2] S. Lehrman, Nature 401 (1999) 517.
[3] P.L. Felgner, T.R. Gadek, M. Holm, R. Roman, H.W. Chan, M. Wenz, J.P. Northrop, G.M. Ringold, M. Danielsen, Proc. Natl. Acad. Sci. USA 84 (1987) 7413.
[4] A.D. Miller, Angew. Chem., Int. Ed. 37 (1998) 1769.
[5] D.W. Pack, A.S. Hoffman, S. Pun, P.S. Stayton, Nat. Rev. Drug Discovery 4 (2005) 581.
[6] C.M. Jewell, D.M. Lynn, Curr. Opin. Colloid Interface Sci. 13 (2008) 395.
[7] M.A. Mintzer, E.E. Simanek, Chem. Rev. 109 (2009) 259.
[8] U. Boas, P.M.H. Heegaard, Chem. Soc. Rev. 33 (2004) 43.
[9] C. Watts, M. Marsh, J. Cell Sci. 103 (1992) 1.
[10] N.S. Templeton, D.D. Lasic, Mol. Biotechnol. 11 (1999) 175.
[11] S. Marchetti, G. Onori, C. Cametti, J. Phys. Chem. B 109 (2005) 3676.
[12] D. Matulis, I. Rouzina, V.A. Bloomfield, J. Am. Chem. Soc. 124 (2002) 7331.
[13] S.M. Melnikov, V.G. Sergeyev, K. Yoshikawa, J. Am. Chem. Soc. 117 (1995) 9951.
[14] R. Dias, S. Mel'nikov, B. Lindman, M.G. Miguel, Langmuir 16 (2000) 9577.
[15] M. Cardenas, T. Nylander, R.K. Thomas, B. Lindman, Langmuir 21 (2005) 6495.
[16] D.M. Zhu, R.K. Evans, Langmuir 22 (2006) 3735.
[17] C. Leal, E. Moniri, L. Pegado, H. Wennerstrom, J. Phys. Chem. B 111 (2007) 5999.
[18] H. Nakanishi, K. Tsuchiya, T. Okubo, H. Sakai, M. Abe, Langmuir 23 (2007) 345.
[19] E. Grueso, F. Sanchez, J. Phys. Chem. B 112 (2008) 698.
[20] J. Zhang, D.J.F. Taylor, P.X. Li, R.K. Thomas, J.B. Wang, J. Penfold, Langmuir 24 (2008) 1863.
[21] S. Gaweda, M.C. Moran, A. Pais, R.S. Dias, K. Schillen, B. Lindman, M.G. Miguel, J. Colloid Interface Sci. 323 (2008) 75.
[22] M. Soliman, S. Allen, M.C. Davies, C. Alexander, Chem. Commun. 46 (2010) 5421.
[23] A.J. Kirby, P. Camilleri, J. Engberts, M.C. Feiters, R.J.M. Nolte, O. Soderman, M. Bergsma, P.C. Bell, M.L. Fielden, C.L.G. Rodriguez, P. Guedat, A. Kremer, C. McGregor, C. Perrin, G. Ronsin, M.C.P. van Eijk, Angew. Chem., Int. Ed. 42 (2003) 1448.
[24] P.C. Bell, M. Bergsma, I.P. Dolbnya, W. Bras, M.C.A. Stuart, A.E. Rowan, M.C. Feiters, J. Engberts, J. Am. Chem. Soc. 125 (2003) 1551.
[25] Y.L. Wang, P.L. Dubin, H.W. Zhang, Langmuir 17 (2001) 1670.
[26] N. Jiang, P.X. Li, Y.L. Wang, J.B. Wang, H.K. Yan, R.K. Thomas, J. Phys. Chem. B 108 (2004) 15385.
[27] C. McGregor, C. Perrin, M. Monck, P. Camilleri, A.J. Kirby, J. Am. Chem. Soc. 123 (2001) 6215.
[28] D. Lleres, J.P. Clamme, E. Dauty, T. Blessing, G. Krishnamoorthy, G. Duportail, Y. Mely, Langmuir 18 (2002) 10340.
[29] L. Karlsson, M.C.P. van Eijk, O. Soderman, J. Colloid Interface Sci. 252 (2002) 290.
[30] N. Jiang, J.B. Wang, Y.L. Wang, H.K. Yan, R.K. Thomas, J. Colloid Interface Sci. 284 (2005) 759.
[31] X.F. Zhao, Y.Z. Shang, H.L. Liu, Y. Hu, J. Colloid Interface Sci. 314 (2007) 478.
[32] S. Bhattacharya, P.V. Dileep, Bioconjugate Chem. 15 (2004) 508.
[33] A. Bajaj, P. Kondaiah, S. Bhattacharya, Bioconjugate Chem. 18 (2007) 1537.
[34] P. Barthelemy, C.A.H. Prata, S.F. Filocamo, C.E. Immoos, B.W. Maynor, S.A.N. Hashmi, S.J. Lee, M.W. Grinstaff, Chem. Commun. (2005) 1261.
[35] V.G. Sergeyev, O.A. Pyshkina, A.V. Lezov, A.B. Mel'nikov, E.I. Ryumtsev, A.B. Zezin, V.A. Kabanov, Langmuir 15 (1999) 4434.
[36] Y.S. Me'nikova, B. Lindman, Langmuir 16 (2000) 5871.
[37] M.A. Kostiainen, H. Rosilo, Chem. – Eur. J. 15 (2009) 5656.
[38] D.J. Welsh, S.P. Jones, D.K. Smith, Angew. Chem., Int. Ed. 48 (2009) 4047.
[39] M.E. Hays, C.M. Jewell, D.M. Lynn, N.L. Abbott, Langmuir 23 (2007) 5609.
[40] M. Sollogoub, S. Guieu, M. Geoffroy, A. Yamada, A. Estevez-Torres, K. Yoshikawa, D. Baigl, ChemBioChem 9 (2008) 1201.
[41] M. Geoffroy, D. Faure, R. Oda, D.M. Bassani, D. Baigl, ChemBioChem 9 (2008) 2382.
[42] A. Diguet, N.K. Mani, M. Geoffroy, M. Sollogoub, D. Baigl, Chem. – Eur. J. 16 (2010) 11890.
[43] Y.C. Liu, A.L.M. Le Ny, J. Schmidt, Y. Talmon, B.F. Chmelka, C.T. Lee, Langmuir 25 (2009) 5713.
[44] A.L.M. Le Ny, C.T. Lee, J. Am. Chem. Soc. 128 (2006) 6400.
[45] J. Andersson, S.M. Li, P. Lincoln, J. Andreasson, J. Am. Chem. Soc. 130 (2008) 11836.
[46] B.A. Cicciarelli, T.A. Hatton, K.A. Smith, Langmuir 23 (2007) 4753.
[47] D.L. Sackett, J. Wolff, Anal. Biochem. 167 (1987) 228.
[48] M.C.A. Stuart, J.C. van de Pas, J. Engberts, J. Phys. Org. Chem. 18 (2005) 929.
[49] C. Dugave, L. Demange, Chem. Rev. 103 (2003) 2475.
[50] X.D. Song, J. Perlstein, D.G. Whitten, J. Am. Chem. Soc. 119 (1997) 9144.
[51] J.M. Kuiper, M.C.A. Stuart, J. Engberts, Langmuir 24 (2008) 426.
[52] R.F. Tabor, R.J. Oakley, J. Eastoe, C.F.J. Faul, I. Grillo, R.K. Heenan, Soft Matter 5 (2009) 78.
[53] Y.Y. Lin, A.D. Wang, Y. Qiao, C. Gao, M. Drechsler, J.P. Ye, Y. Yan, J.B. Huang, Soft Matter 6 (2010) 2031.
[54] Y.Y. Lin, X.H. Cheng, Y. Qiao, C.L. Yu, Z.B. Li, Y. Yan, J.B. Huang, Soft Matter 6 (2010) 902.
[55] Y.Y. Lin, Y. Qiao, P.F. Tang, Z.B. Li, J.B. Huang, Soft Matter 7 (2011) 2762.
[56] T. Hayashita, T. Kurosawa, T. Miyata, K. Tanaka, M. Igawa, Colloid Polym. Sci. 272 (1994) 1611.
[57] C.T. Lee, K.A. Smith, T.A. Hatton, Macromolecules 37 (2004) 5397.
[58] H. Liu, J. Gapinski, L. Skibinska, A. Patkowski, R. Pecora, J. Chem. Phys. 113 (2000) 6001.
[59] R.S. Dias, J. Innerlohinger, O. Glatter, M.G. Miguel, B. Lindman, J. Phys. Chem. B 109 (2005) 10458.
[60] A. Mitra, T. Imae, Biomacromolecules 5 (2004) 69.
[61] L.S. Lerman, J. Mol. Biol. 3 (1961) 18.
[62] S.J. Eastman, C. Siegel, J. Tousignant, A.E. Smith, S.H. Cheng, R.K. Scheule, Biochim. Biophys. Acta – Biomembr. 1325 (1997) 41.
[63] Y.H. Xu, S.W. Hui, P. Frederik, F.C. Szoka, Biophys. J. 77 (1999) 341.

[64] R.C. MacDonald, G.W. Ashley, M.M. Shida, V.A. Rakhmanova, Y.S. Tarahovsky, D.P. Pantazatos, M.T. Kennedy, E.V. Pozharski, K.A. Baker, R.D. Jones, H.S. Rosenzweig, K.L. Choi, R.Z. Qiu, T.J. McIntosh, Biophys. J. 77 (1999) 2612.
[65] Y.H. Ding, L. Zhang, J. Xie, R. Guo, J. Phys. Chem. B 114 (2010) 2033.
[66] W. Chen, N.J. Turro, D.A. Tomalia, Langmuir 16 (2000) 15.
[67] A. Rodriguez-Pulido, F. Ortega, O. Llorca, E. Aicart, E. Junquera, J. Phys. Chem. B 112 (2008) 12555.
[68] C. Cabaleiro-Lago, M. Nilsson, O. Soderman, Langmuir 21 (2005) 11637.
[69] J.W. Park, H.J. Song, J. Phys. Chem. 93 (1989) 6454.
[70] Y.P. Wang, N. Ma, Z.Q. Wang, X. Zhang, Angew. Chem., Int. Ed. 46 (2007) 2823.
[71] P.J. Zheng, C. Wang, X. Hu, K.C. Tam, L. Li, Macromolecules 38 (2005) 2859.
[72] X. Chen, L. Hong, X. You, Y.L. Wang, G. Zou, W. Su, Q.J. Zhang, Chem. Commun. (2009) 1356.
[73] A. Gonzalez-Perez, J. Carlstedt, R.S. Dias, B. Lindman, Colloids Surf., B – Biointerfaces 76 (2010) 20.
[74] A. Gonzalez-Perez, R.S. Dias, T. Nylander, B. Lindman, Biomacromolecules 9 (2008) 772.